Agronomy Research **15**(S1), 1072–1083, 2017

A dynamic model of electric resistor's warming and its verification by micro-thermocouples

M. Linda, G. Künzel and M. Hromasová*

Czech University of Life Sciences in Prague, Faculty of Engineering, Department of Electrical Engineering and Automation, Kamýcká 129, CZ165 21 Prague, Czech Republic
*Correspondence: hromasova@tf.czu.cz

Abstract. The object of research is a resistor, a real electronic component, loaded by constant or impulse power. As a first approximation, resistor follows 1st order dynamic system, i.e. heating of the hottest spot on its surface is exponential to the power increase. The validity of this model is confirmed by measurements in a constant power loading regime. In an impulse power loading, it is only valid when the pulse duration approaches time constant of the resistor. The aim of this article is to show more credible model warming of the resistor, which is valid even for the case of pulse duration (ms) much shorter than the time constant of the resistor. The model can reveal an overload which does not lead to destruction of the resistor. Dynamic model of the resistor is based on its construction. Typically, an insulating ceramic rod is coated with a resistive layer connected with outlet wires on both sides, all being coated with insulating lacquer layer. The resistive layer is a source of heat flow. Formulation of the model comes from general power balance in a form of three differential equations and it is solved using Scilab. The input variable is the impulse power and the outputs are temperature changes in the ceramic rod, the resistive layer and the lacquer layer, compared to the ambient temperature. The simulation allows to determine solutions for various parameters including very short power pulses, which are confirmed experimentally.

Key words: load factor, model, resistor, thermocouple, warming.

INTRODUCTION

Resistors with power loading mostly between 0.1–2 W, or alternatively power resistors with power handling capacity of 10–100 W are the significant heat-sources in electric devices. Since the electric power in the resistor changes into a heat flux, and thus it's operated at a loss, this passive electrical component, from the heat transfer point of view, is probably the most interesting, and in many cases, also the solution of the heat and temperature field (O'Sullivan & Cotterell, 2001; Song et al., 2016). It is necessary, when designing the electrical devices to project correctly a nominal value of the resistor and its type with regard to its power load. In case of inappropriate choice the component might be destroyed.

This paper deals with the formulation, design, and experimental verification of a dynamic model of a resistor in a pulse-loaded mode by the power. A typical application would be reduction of a capacitor's charging current, soft starter of transformer, or an inrush current suppression of an induction motor (Osmanaj & Selimaj, 2009).

The object of the research is a resistor with a metal-oxide layer 100 Ω and with power of 2 W (type MO–300) (GMElectronic, 2008). The parts manufacturer usually states the pulse load only for special power and pulse resistors (Shin et al., 2009). A Graph of an energy absorption 'energy capability' is provided for short pulses of 100 ms. So called overload characteristic is provided for longer pulses. A limitation based on shock wave test is used for pulses < 1 ms (Batal et al., 2014).

Understanding the damage mechanism of the metal-oxide resistor is shown e.g. in (ROHM, 2012). When power overload occurs, firstly there is an oxide reduction on metal, which results in a slight decrease of the nominal resistance. Longer overload leads to a melting of resistive layer, or cracking and melting in a layer of ceramic rod, or in resistor's coating, until the resistive layer is damaged. The last phase of resistive layer melting is characterized by a significant resistance increase. The component is inoperable and needs to be replaced (Hromasová & Linda, 2016).

Dynamic model of the resistor is based on its structural arrangement. Formulation of electro thermal system respects the power balance of a resistor's part. The simplest model is a first-order model with a time constant substantially greater than the duration of power pulses (Böckh & Wetzel, 2012; Contento & Semancik, 2016). For a very short pulses in ms, the validity of this model is limited, as it's demonstrated by measurements using micro thermocouples (Degenstein et al., 2007). Therefore a more complex dynamic model was designed, which reflects better the warming of the ceramic rod, the resistance layer, and the lacquer layer. After parameter identification and verification, based on measurements, it is possible to simulate on PC model a complex behaviour of the resistor in the pulse mode and determine the conditions of acceptable overload capacity without destruction of the component.

MATERIALS AND METHODS

A typical resistor is usually comprised of a ceramic rod (sometimes tubes), on which surface is applied an electrically conductive resistive layer, which is connected at both ends e.g. by copper wire outlets. This layer is covered by a lacquer insulation layer. From the cybernetic viewpoint, we can see the resistor as a dynamic electro thermal system, which input is loaded constant or pulsed electrical power P (W) and the output is temperature ϑ (°C) (Fig. 1). The resistive layer is a source of a heat flux, which is equivalent to the electric power. Static model of a heat transfer between the heat source and the environment does not define the structure of the resistor. The main problem is that there is no part on the resistor's construction, which would correspond to a thermal circuit's node with temperature ϑ. Therefore the practice of measuring temperature ϑ got stabilised (warming determination given the ambient temperature ϑ_0) at the hottest point of the resistor, usually in the middle of the cylindrical coating (Fig. 2). Warming $\Delta\vartheta$ (1) in a steady state is considered as directly proportional to the power P on the resistive layer.

$$\Delta\vartheta = \vartheta - \vartheta_0 \tag{1}$$

Figure 1. Block diagram of the power-loaded resistor (Linda & Hromasová, 2016a).

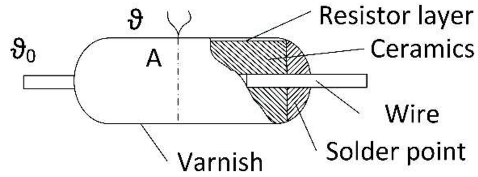

Figure 2. Indication of areas suitable for measuring the resistor's surface temperature (Linda & Hromasová, 2016a).

If we disregard the convention as well as radiation from the coating's surface, the dynamic model of a second-order will be sufficient, based on the ideas of heat flux branching on the resistor according to a replacement RC heat circuit with two loops. Repeated measurements of the warming transition characteristics and their identification showed, that this noncascade model of second-order satisfies, with an adequate accuracy, a real resistor's mode of the rectangular-pulsed power input signals. Warming transition characteristics in standardized form $h(t)$ have a form of (2) (Linda & Hromasová, 2016a)

$$h(t) = 1 - A_1 \exp\left(-\frac{t}{T_1}\right) - (1 - A_1)\exp\left(-\frac{t}{T_2}\right) = \frac{\Delta\vartheta(t)}{\Delta\vartheta_{jm}} \qquad (2)$$

where: A_1 –constant ratio; t –time, s; T_1, T_2 –time constant, s; $\Delta\vartheta(t)$ –immediate warming, °C; $\Delta\vartheta_{jm}$ –nominal value of warming, °C.

The model can be quantified by a regression method, where we determine time constants T_1, T_2 for each sample or type resistor and a constant ratio A_1 for the minimum value of the sum of squared deviations. In the model (2) is a smaller time constant T_1, that always corresponds with a product of heat capacity of the lacquer layer and with thermal resistance between the layer and the environment, while $T_2 > T_1$ is given by the product of heat capacity of the ceramic rod, eventually by the outlets and the thermal resistance between the resistive layer and the surroundings.

Each energy (power) balance is the mathematical expression of the law of conservation of energy (power). Simplified wording of the equation of conservation is (3) (Linda & Hromasová, 2016a; 2016b)

$$\mathrm{INPUT} + \mathrm{SOURCE} = \mathrm{OUTPUT} + \mathrm{ACCUMULATION} \qquad (3)$$

Heat balance of the object's unit volume at the propagation of heat is then (4)

$$\begin{bmatrix}\text{Input}\\ \text{heat flux}\\ \text{into the}\\ \text{element}\end{bmatrix}+\begin{bmatrix}\text{External}\\ \text{source}\\ \text{of heat flux}\end{bmatrix}=\begin{bmatrix}\text{Output}\\ \text{heat flux}\\ \text{from the element}\end{bmatrix}+\begin{bmatrix}\text{Time change of}\\ \text{the inner energy}\\ \text{in the element,}\\ \text{i. e. accumulation}\end{bmatrix} \tag{4}$$

This general approach to the creation of resistor's electro thermal model leads to a system of first-order ordinary differential equations with lumped constant parameters. We compile a power balance for each layer and also the ceramic rod. Block diagram of the distribution of individual heat fluxes *q (w)* (q_i, q_{12}, q_{13}, q_{01}, q_{02}) between the individual elements of the real resistor is on Fig. 3.

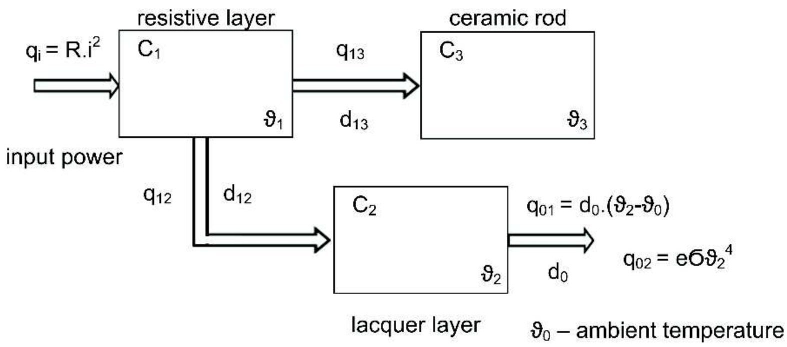

Figure 3. The block diagram of the distribution of heat fluxes.

Power balance of the resistive layer is described by Eq. (5)

$$Ri^2 = C_1\frac{d\vartheta_1}{dt} + d_{12}(\vartheta_1 - \vartheta_2) + d_{13}(\vartheta_1 - \vartheta_3) \tag{5}$$

where: R –electrical resistance of the examined object, Ω; i –the electric current, A; C_1 –the heat capacity of the resistive layer, J K^{-1}; d_{12}, d_{13}*3* –coefficients of heat transfer from the resistive layer to the surface coating and the ceramic rod, W K^{-1}; $\vartheta_1(t)$, $\vartheta_2(t)$, $\vartheta_3(t)$ –the temperatures of the resistive layer, lacquer layer and the ceramic rod, °C.

Power balance of the lacquer layer is described by Eq. (6)

$$d_{12}(\vartheta_1 - \vartheta_2) = C_2\frac{d\vartheta_2}{dt} + d_0(\vartheta_2 - \vartheta_0) + e\sigma S\vartheta_2^4 \tag{6}$$

where: C_2 –the heat capacity of the lacquer layer, J K^{-1}; ϑ_0 = 24 °C –ambient temperature, °C; $e \le 1$ emissivity of the resistor's surface; $\sigma = 5.78\ 10^{-8}$ Wm^{-2}K^{-4} Stefan-Boltzmann constant; S –the surface size of resistor's cylinder; m^2.

Due to the fourth power of temperature $\vartheta_2(t)$ is the differential equation nonlinear. Heat flux q_{02}, which can be emitted during radiation from the surface, is determined by the Stefan-Boltzmann law. Analogous power balance of the resistor's ceramic rod is expressed by the Eq. (7)

$$d_{13}(\vartheta_1 - \vartheta_3) = C_3\frac{d\vartheta_3}{dt} \tag{7}$$

where: C_3 –the rod's thermal capacity, J K^{-1}.

The resistor model is loaded by the input electric power, which is represented by a formula $P = Ri^2$and for constant values of the resistance as well as the current is also constant. If we examine the pulse-loading mode of the resistor, we need to supply periodic rectangular pulses with a pulse power P, the duration t_1 (s) with the time period T (s) to define the following parameters according to Fig. 4. (O'Sullivan & Cotterell, 2001).

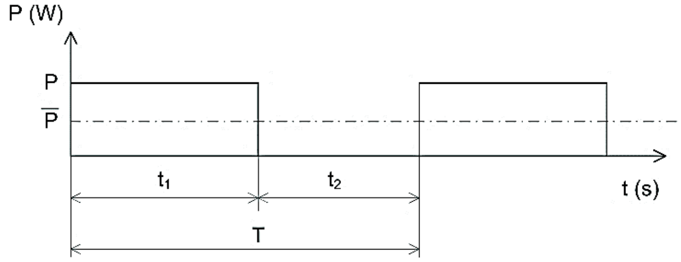

Figure 4. The power pulse.

Load factor z (-, %)

$$z = \frac{t_1}{T} \tag{8}$$

Medium power $\bar{P}$ (W)

$$\bar{P} = \frac{P_1 t_1}{T} = P_1 z \tag{9}$$

Medium warming $\Delta\bar{\vartheta}$ (°C) in a steady state

$$\Delta\bar{\vartheta} = k\bar{P} = kP_1 z \tag{10}$$

where: k –a constant corresponding to a thermal resistance in a steady state, K W^{-1}.

A warming $\Delta\vartheta_1$ given by continuous power P_1

$$\Delta\vartheta_1 = kP_1 = \frac{k\bar{P}}{z} = \frac{\bar{\vartheta}}{z} \tag{11}$$

These formulas serve as an evaluation of the measured time courses of warming of the particular resistors, but also can be used for a pulse mode of the resistor's dynamic model.

For the model quantification, we need to know the values of heat capacities, which can be calculated using the dimensions of the resistor, cubic density ρ_m (kg m^{-3}) and specific heat C (J kg^{-1}K^{-1}). The thickness of the resistive layer of the resistor MO-300 100 Ω was measured using a microscope, and it is about 2 microns. The length of the resistor $l = 11$ mm and its radius $r = 2$ mm can be determined from the data (O'Sullivan & Cotterell, 2001). The values of heat capacities of the individual resistor layers are shown in Table 1.

The heat transfer coefficients were identified by comparing with the conducted experiment. Three pieces of the same resistor were chosen, and each of them was continuously loaded by power of 2 W five times. During this, the surface temperatures in the middle of the resistor were also measured. To determine the searched-for parameters, we used a method of least squares of the difference between the measured temperature and the model's temperature. Calculated values of the heat transfer coefficients are in Table 2.

Table 1. Calculated parameters of heat capacity

Layer	Label	Heat capacity (J K^{-1})
Resistive	C_1	1.11 x 10^{-3}
Lacquer	C_2	9.93 x 10^{-3}
Ceramic	C_3	314 x 10^{-3}

Table 2. Averages of calculated coefficients

Parameters	Sample 1	Sample 2	Sample 3
d_{12} (W K^{-1})	0.763	0.758	0.757
d_{13} (W K^{-1})	0.254	0.254	0.253
d_0 (W K^{-1})	0.008	0.008	0.009

In a differential energy balance equations the individual elements participate in a total warming unevenly. By so called Sensitivity analysis we can determine the effect of changes of individual parameters in the equations on a maximum warming of the resistor, and possibly decide, what elements need not be considered when dimensioning the resistors by short repetitive pulses.

Relative sensitivity function S_a^y is defined as the ratio (12)

$$S_{a_{i_3}}^{y} = \frac{\frac{dY}{Y}}{\frac{da_i}{a_i}} = \frac{dY}{da_i}\frac{a_i}{Y} \qquad (12)$$

We expect a linear dependence of the relative output variable $\frac{dY}{Y}$ on the relative change of each individual parameter. In our case, the function Y represents a maximum possible temperature in the resistive layer. The relative change of the parameter was chosen $\frac{da_i}{a_i} = 0.01$ ie. 1%.

RESULTS AND DISCUSSION

The complete mathematical model expressed by the Eqs (5–7) was created in Scilab Xcos and its block diagram is on Fig. 5.

The computer model graphically displays the temperature curses $\vartheta_1(t)$resistive layer, $\vartheta_2(t)$ lacquer layer and $\vartheta_3(t)$ ceramic layer for different variants of the entered parameters from Table 1 and Table 2. for the constant as well as a pulse-loaded power entering into the resistor.

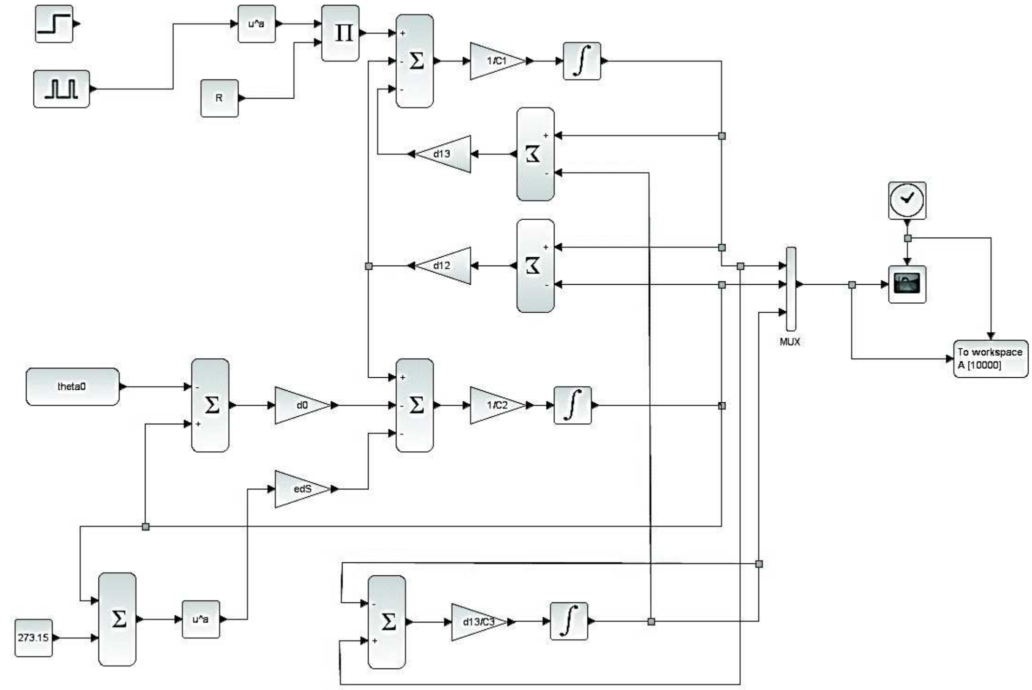

Figure 5. Block diagram of models in Scilab-Xcos.

Fig. 6 show temperature response to steady state. Input signal is step function of electrical current. Final temperature of response is 77.4 °C and electrical current is 70 mA.

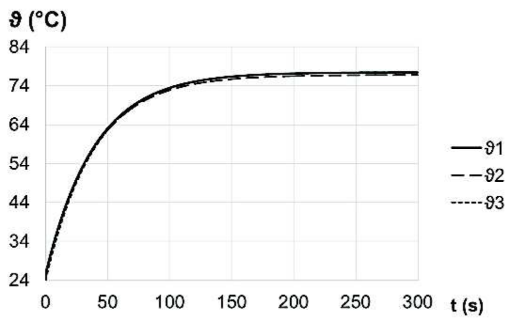

Figure 6. The temperature waveform $i = 0.07$ A.

Fig. 7 show temperature waveform for sample 1 (Fig. 7, a), 2 (Fig. 7, b) and 3 (Fig. 7, c) with constant current 0.14 A, time to the period 14 ms and pulse duration 7 ms.

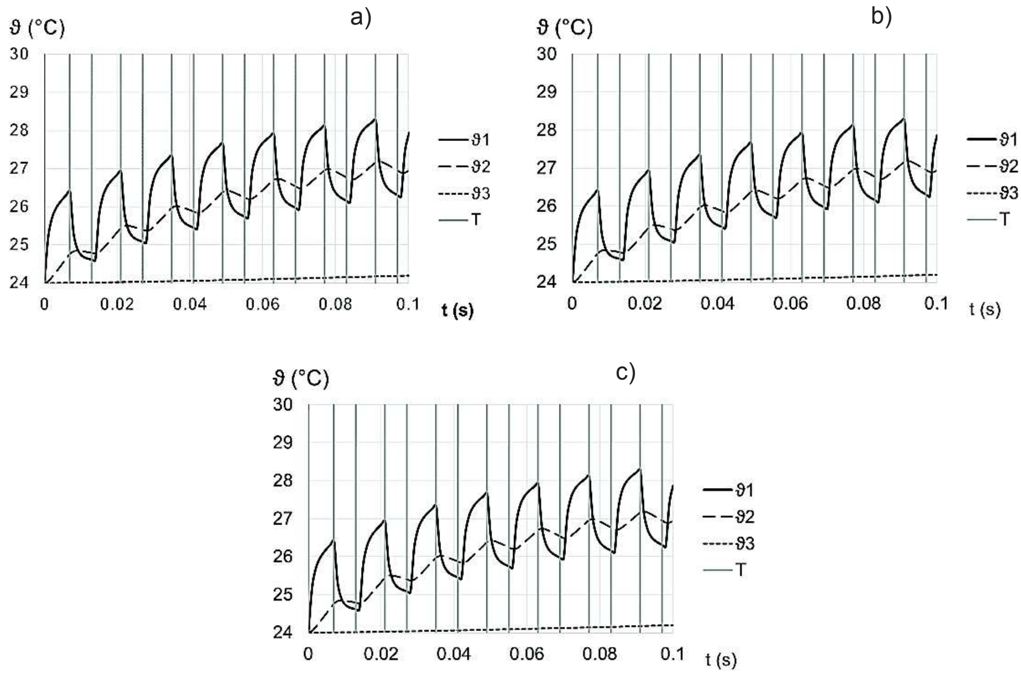

Figure 7. The temperature waveform –sample 1 a), 2 b) and 3 c), $T = 14$ ms, $t_1 = 7$ ms.

Fig. 7, a), 8, a), 8, b show temperature waveform for sample 1 with constant current 0.14 A, time to the period was changed to a value 2 ms, 14 ms and 100 ms and pulse duration was changed to a value 1 ms, 7 ms and 50 ms.

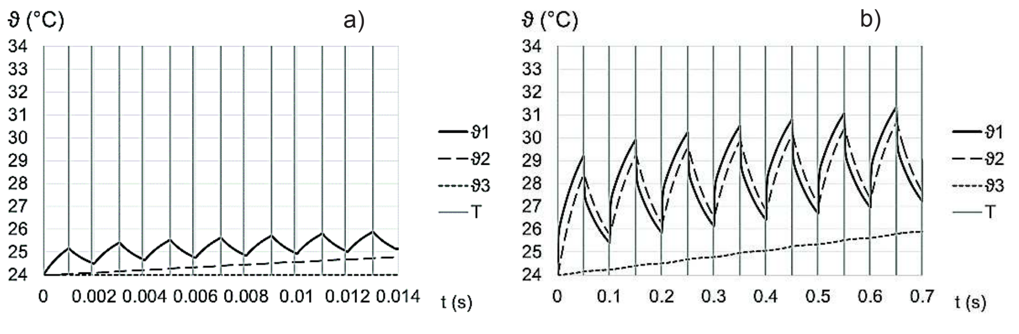

Figure 8. The temperature waveform –sample 1, a) $T = 2$ ms, $t_1 = 1$ ms and b) $T = 100$ ms, $t_1 = 50$ ms.

Fig. 9 shows temperature waveform sample 1 with constant current 0.42 A, time to the period was changed to a value 2 ms, 14 ms and 100 ms and pulse duration was changed to a value 1 ms, 7 ms and 50 ms.

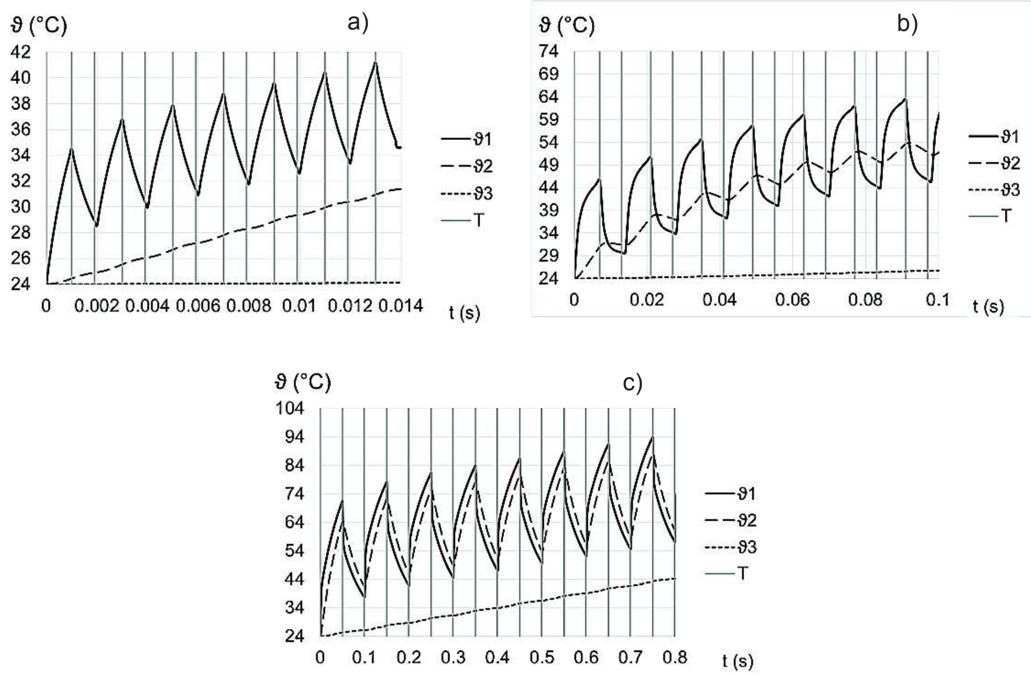

Figure 9. The temperature waveform –sample 1, a) $T = 2$ ms, $t_1 = 1$ ms; b) $T = 14$ ms, $t_1 = 7$ ms; c) $T = 100$ ms, $t_1 = 50$ ms.

Fig. 10 shows temperature waveform sample 1 with constant current 1.4 A, time to the period 32 ms and pulse duration 16 ms.

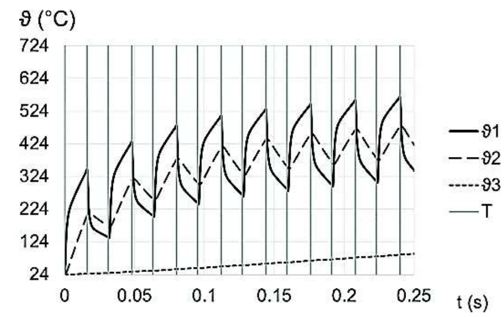

Figure 10. The measured waveform –sample 1, $T = 32$ ms, $t_1 = 16$ ms.

It is noticeable from the graphical dependencies of the sensitivity function on parameters' changes at a constant amplitude of the current of 140 m A with rectangular pulses with duration of 0.8 ms, that the warming sensitivity on the thermal capacity change C_1 (resistive layer) is at the highest. At even shorter pulses is not sufficient to fully explore the ability to accumulate the created heat energy. Sensitivity to parameter C_2 (insulating layer) is the highest for 51 ms pulses. The biggest impact on warming, however, has the heat capacity of the ceramic rod C_3, which is higher by 2 orders of magnitude, but it applies itself at longer pulses. The coefficient d_{12} has a high sensitivity when the effect of the thermal capacity of the resistive and the covering insulating layer manifest itself the most. Parameters d_{13} and d_0 have a higher sensitivity by an order of magnitude than d_{12} and their course corresponds with the sensitivity to the thermal capacity C_3.

The simulation of the created model shows that temperature of the insulation layer during short pulses of 1–7 ms lags behind the reached temperature of the resistive layer until the pulse is of 50 ms duration. The ceramic rod does not warm up close to the temperature of the resistive layer, even when pulse-loaded for an order of magnitude of seconds. The simulated course while the temperatures are higher than ca 700 °C, is however unrealistic because the resistive layer was, without a doubt, destructed, as shown in comparisons of the measurement results and the model.

During the loading by the current of 1.4 A and by pulse of 16 ms (50% cycle), the destruction does occur in the examined resistor with resistance of 100 Ω and with maximum allowable continuous power-loading of 2 W. The maximum temperature of the resistive layer in time 0.24 s was identified at 540 °C, the temperature of the lacquer layer at 450 °C and of the ceramic rod at 86 °C.

Measuring of the resistors when the pulse-loading was underway using a created measuring apparatus in a free space. The influence of the environment on short pulses is minimal. The heat from the resistive layer does not suffice to warm up significantly the surface layer of the resistor. Resistors were loaded by pulses of 5 ms duration. Between pulses was the corresponding pulse energy -30 s for the energy of 1 J, because the resistor cooled down to the ambient temperature. At the end of the cooling time was the resistance measured with a multimeter connected by a 4-wire method to the resistor. Resistance does not change its value at first. Initial temperature of the resistances differ in individual pieces, which is in accordance with tolerances stated in the manufacturers' catalogue. The damage mechanism of the metal-oxide resistor occurs successively in three phases, as shown in Table 3, which is developed on the basis of a statistical evaluation of 12 measurements. The resistor was always damaged near the centre of the ceramic rod. Destruction was associated with formation of an electric arc at the point of damage.

Table 3. Individual phases of resistor's damage

Phases	Impulse of current (A)	Pulse of energy (J)
Reduction O_2	1.10–1.30	0.6–0.9
Fusion resistive layer	1.65–1.95	1.6–2
Destruction	1.90–2.20	1.8–2.6

The accuracy of the model can be demonstrated by comparing the warming transition characteristic of the resistor's model $\Delta\vartheta_2(t)$ and the measured warming transition characteristic in the centre of the real resistor's surface, provided that the input power pulses are in both cases the same. The conditions of the correct and sufficiently accurate measurement of the very rapid time courses of temperatures using micro thermocouples are stated in (Hromasová & Linda, 2016; Linda & Hromasova, 2016a, 2016b). Given that, the measurement of the warming using these sensors has a non-zero error, the model's maximum error of 1.5% can be determined based on the statistical processing of 150 samples of transition characteristics.

CONCLUSIONS

Using the power balance, we formulated a mathematical model of a heat transfer in three subsystems of the resistor as a system of differential equations of first-order. Computer model in Scilab Xcos was created after adjusting. The computer model graphically displays the temperature curses $\vartheta_1(t)$, $\vartheta_2(t)$ a $\vartheta_3(t)$ for different variants of the entered parameters from Table 1 and Table 2. for the constant as well as a pulse-loaded power entering into the resistor.

We obtain more information about the loaded resistor from the computer model than during the surface temperature measurement eg. using thermocouples or pyrometers. Usability of the model in practice is possible, based on the experimental identification of the model's parameters. The measurement is irreplaceable, however it only observes how the temperature changes in time but does not explain the physical nature of correlations among quantities.

Comparison of results of the model's behaviour and the measurements show us what impulses can be used to load the resistor, in order not to exceed the maximum allowable warming from the dimensioning viewpoint. The destruction of the component occurs when the temperature of the resistive layer is at about 700 °C.

The mentioned methodology may be used for research of thermal dynamics in more complex components (capacitors, diodes, transistors, thyristors, or integrated circuit), where is certainly necessary to address the related issue of cooling.

REFERENCES

Batal, M.A., Nashed, G. & Jneed, F.H. 2014. Conductivity and thermoelectric properties of nanostructure tin oxide thin films. *Journal of the Association of Arab Universities for Basic and Applied Sciences* **15**, 15–20.

Böckh, P. von. & Wetzel, T. 2012. *Heat transfer: basics and practice*. Springer, 276 p.

Contento, N.M. & Semancik, S. 2016. Thermal characteristics of temperature-controlled electrochemical microdevices. *Sensors and Actuators B: Chemical* **225**, 279–287.

Degenstein, T., Günter, M., Keller, A. & Winner, H. (n.d.). 2007. Dynamic measurement of the temperature of electro conductive objects used for the example of a wheel brake. AMA Service GmbH, 2007, **A1**(4), 1–5.

GMElectronic. 2008. Power metal film resistor. Retrieved from http://www.gme.cz/

Hromasová, M. & Linda, M. 2016. Analysis of rapid temperature changes. *Agronomy Research* **14**(3), 768–778.

Linda, M. & Hromasová, M. 2016a. Analysis of rapid temperature changes of the object with higher thermal constant. In. *Proceeding of 6th international conference on trends in agricultural engineering*, Jelgava. pp. 366–374.
Linda, M. & Hromasová, M. 2016b. Model analysis of temperature sensors. In *Engineering for Rural Development*, Jelgava. pp. 566–573.
O'Sullivan, D. & Cotterell, M. 2001. Temperature measurement in single point turning. *Journal of Materials Processing Technology* **118**(1), 301–308.
Osmanaj, S.F. & Selimaj, R.A. 2009. Thermal Analysis Of Electrical Machines. *TMT*, 16–21.
ROHM. 2012. ROHM Semiconductor. Retrieved from http://www.rohm.com/products/databook/r/pdf/r_siyoujou.pdf
Shin, D., Kim, J., Chang, N., Choi, J., Chung, S.W. & Chung, E.-Y. 2009. Energy-optimal dynamic thermal management for green computing. In *Proceedings of the 2009 International Conference on Computer-Aided Design - ICCAD '09* (p. 652). New York, New York, USA: ACM Press.
Song, H., Zhan, X., Li, D., Zhou, Y., Yang, B., Zeng, K. & Tang, J. 2016. Rapid thermal evaporation of Bi2S3 layer for thin film photovoltaics. *Solar Energy Materials and Solar Cells* **146**, 1–7.